



Publisher: Association of Metallurgical Engineers of Serbia

Metallurgical and Materials Data

www.metall-mater-data.com



## Quantitative analysis of mechanically alloyed CuZrB powders

Marko Simić<sup>1,2\*</sup>, Aleksa Luković<sup>1,2</sup>, Gvozden Jovanović<sup>3</sup><sup>1</sup> University of Belgrade, Vinča Institute of Nuclear Sciences - National Institute of the Republic of Serbia, Department of Materials, Belgrade, Serbia<sup>2</sup> University of Belgrade, Vinča Institute of Nuclear Sciences - National Institute of the Republic of Serbia, Center of Excellence "CEXTREME LAB, Belgrade, Serbia<sup>3</sup> Institute for Technology of Nuclear and Other Mineral Raw Materials, 86 Franchet d'Esperey St., Belgrade, Serbia

### ARTICLE INFORMATION :

<https://doi.org/10.56801/MMD44>

Received: 13 December 2024

Accepted: 25 February 2025

Type of paper: Research paper



Copyright: © 2024 by the authors, under the terms and conditions of the Creative Commons Attribution (CC BY) license (<https://creativecommons-mons.org/licenses/by/4.0/>).

### ABSTRACT

Copper matrix composites are proving to be a suitable match for the present engineering needs of the market where higher temperature resistance and good microstructural stability are required. Powder metallurgy technique was used to procure the powder mixture, Cu-2Zr-0.6B (wt.%). Different mechanical alloying (MA) parameters were examined with the main focus on time, ranging from 10 h to 40 h. SEM analysis was employed to determine structural and morphological changes of the mechanically alloyed powder mixture. MIPAR image analysis software was used to complete the quantitative analysis of the mechanically alloyed CuZrB powders. Changes in size and shape of powder particles were determined during up to 40 h of MA with key points after every 10 h. It was concluded that the powder particle size decreases as the MA time increases. With the increase in MA time the area of each particle decreases due to the dominant plastic deformation mechanisms as particles undergo high forces through ball-particle-ball and wall-particle-ball collisions during the MA process.

**Keywords:** copper based composites, powder metallurgy, mechanical alloying, MIPAR, image analysis.

### 1. Introduction

Over the past few years, there has been a noticeable surge in the popularity of metal matrix composites (MMC), because of their significantly enhanced and advanced properties compared to the traditional materials (Jamwal et al., 2020). Copper (Cu) is the most commonly added element to alloys in the form of powder, mainly because it's affordable, easily accessible, and has the ability to enhance the properties of the alloys (Zhang et al., 2015). Above mentioned enhancements in copper-based MMCs are proved to be a suitable match for the present engineering needs of the market where higher temperature resistance and good microstructural stability are required (Jamwal et al., 2020), (Zhang et al., 2015), (Gautam et al., 2018), (Srivatsan et al., n.d.), (Chawla & Chawla, n.d.), (Wong-Ángel et al., 2014), (Şap et al., 2021). Copper-based MMCs are widely employed in various applications including thermal management, electronics, submarine components, aerospace and defence, walls of fusion reactors, gas turbine blades, niobium-based superconductors, medical devices, automotive parts, and structural components (Jamwal et al., 2020), (Srivatsan et al., 2000), (Chawla & Chawla, n.d.), (Şap et al., 2021), (Suneev Anil Bansal et al., n.d.), (Ružić et al., 2014), (Shang et al., 2014), (Malaki, 2021).

One of the main reasons that CuZrB composite materials are attracting more and more interest is their unique combination of properties, such as combination of high strength and excellent electrical conductivity. Processing technique plays a major role and influences the properties of these composite materials (Shaik & Golla, 2019).

Traditionally, the majority of copper-based MMCs have been predominantly manufactured through powder metallurgy (PM) process (Alkindi et al., 2023). As processing techniques advance sustainably, the PM route has gained widespread popularity owing to its strong sustainability, precise capabilities, and exceptional dimensional accuracy, all while minimizing scrap waste during the fabrication process (Alkindi et al., 2023), (Wang et al., 2023).

In the PM process, metal powders are mixed with ceramic particles, compacted, and then sintered to create the final composite (Eessaa et al., 2023), (Pingale et al., 2021), (Paul et al., 2023), (Shaik et al., 2021), (Akhtar et al., 2018). This method enables precise control over factors like the size, distribution, and arrangement of ceramic particles within the metal matrix (Shaik et al., 2021). This allows the optimization of the mechanical, electrical, and optical properties of the composite material (Akhtar et al., 2018).

The MA process is influenced by several critical factors that play essential roles in producing uniform materials (Wu et al., 2023), (El-Eskandarany, 2001), (Prasad Yadav et al., 2012). The core process within a mill aimed at generating high-quality powders with controlled microstructures involves the repetitive sequence of welding, fracturing

\* Corresponding author.

E-mail address: [marko.simic@vin.bg.ac.rs](mailto:marko.simic@vin.bg.ac.rs) (Marko Simić).

and subsequent re-welding of a mixture of diffusion-coupled powders. Establishing the right balance between fracturing and cold welding is pivotal for achieving successful MA (Cai et al., 2023).

It's widely recognized that the properties of the MA powders as the final product, including aspects like particle size distribution, disorder or amorphization degree, and stoichiometry, hinge on the milling conditions (Taha et al., 2019). Therefore, the better the control and monitoring of these conditions, the higher the quality of the final product. The most important factors that need to be taken into account include time, types of milling media, atmosphere, milling media-to-powder weight ratio and the type of mills used (Suryanarayana, 2022).

The reason these composite materials are studied mostly relies on their potential to enhance the mechanical, thermal, and electrical properties of copper-based materials. The addition of zirconium and boron refine grain structure, improves strength, and enhances thermal stability, making CuZrB powders valuable for high-performance applications in aerospace, electronics, and structural materials.

In this study, MA in ball mill in order to obtain the CuZrB composite materials is assessed. Different times of MA were chosen for this particular study: 10 h, 20 h, 30 h, and 40 h for a ball-to-powder ratio of 10:1. A quantitative analysis of obtained composite powders was provided and discussed.

## 2. Materials and methods

The initial copper powder had a particle size of  $\sim 15 \mu\text{m}$  (99.5% pure), zirconium  $\sim 1 \mu\text{m}$  (99.5% pure), and boron  $\sim 0.083 \mu\text{m}$  (97% pure). The Cu-2Zr-0.6B (wt.%) mixture was homogenized for 1 h in a Turbula shaker mixer type T2C. The MA process followed homogenization, has been done in the same Turbula mixer with the following process parameters: stainless steel balls with 6 mm diameter, ball-to-powder wt. ratio 10:1, inert argon atmosphere, MA time from 10 h to 40 h (10 h increment), and rotation speed of 330 rpm.

Scanning electron microscopy (SEM) analyses performed using the JEOL-JSM 5800LV microscope, was used to determine the influence of the MA time on the microstructural and morphological changes of the

CuZrB powder mixtures. Materials Image Processing and Automated Reconstruction (MIPAR™) image analysis software was used to complete the quantitative analysis of the mechanically alloyed CuZrB powders (Sosa et al., 2014).

## 3. Results and discussion

Using the MIPAR image analysis software to do the quantitative analysis of the SEM images that we have made, provided us with valuable data on the powders that have been previously mechanically alloyed. As we know, the MA process is the focal point of producing CuZrB composite powders and as a result different parameters were examined. The most important factor chosen for this study is the MA time. Four different MA times were picked for the Cu-2Zr-0.6B powder mixture: 10 h, 20 h, 30 h, and 40 h. MIPAR software provides essential quantitative data that is crucial for understanding the MA process better. For this study data about caliper diameter (largest line length that fits across each feature), area (area of each particle), minimum diameter (smallest line length between two tangential parallel lines), and equivalent diameter (diameter of each feature if each was circle of same area) were provided for all samples.

The SEM images analyzed using this software are provided for all 4 times in relation with the caliper diameter (Figure 1). With the increase in MA time, the shape of powder particle drastically changes (from a round shape to a pancake shape) where the size of caliper diameter increases to a certain point, as the dominant mechanism is welding of the particles. After that point is passed, the caliper diameter continues to decrease as the dominant mechanism is particle breakage.

Figure 2. shows area analyzed for Cu-2Zr-0.6B powders after different MA time. It can be seen that for 10 h of MA, most particles have an area lower than  $2000 \mu\text{m}^2$ . There are less particles with bigger areas and a few particles with the area of  $6.000 \mu\text{m}^2$  -  $10.000 \mu\text{m}^2$ . A similar trend can be seen for 20 h of MA. Most particles have an area lower than  $1000 \mu\text{m}^2$ . There is a comparable number of particles with the area from  $1.000$  to  $2.000 \mu\text{m}^2$ . There are far less particles with the area of  $4.000$ - $5.000 \mu\text{m}^2$ . We can see that due to longer milling times

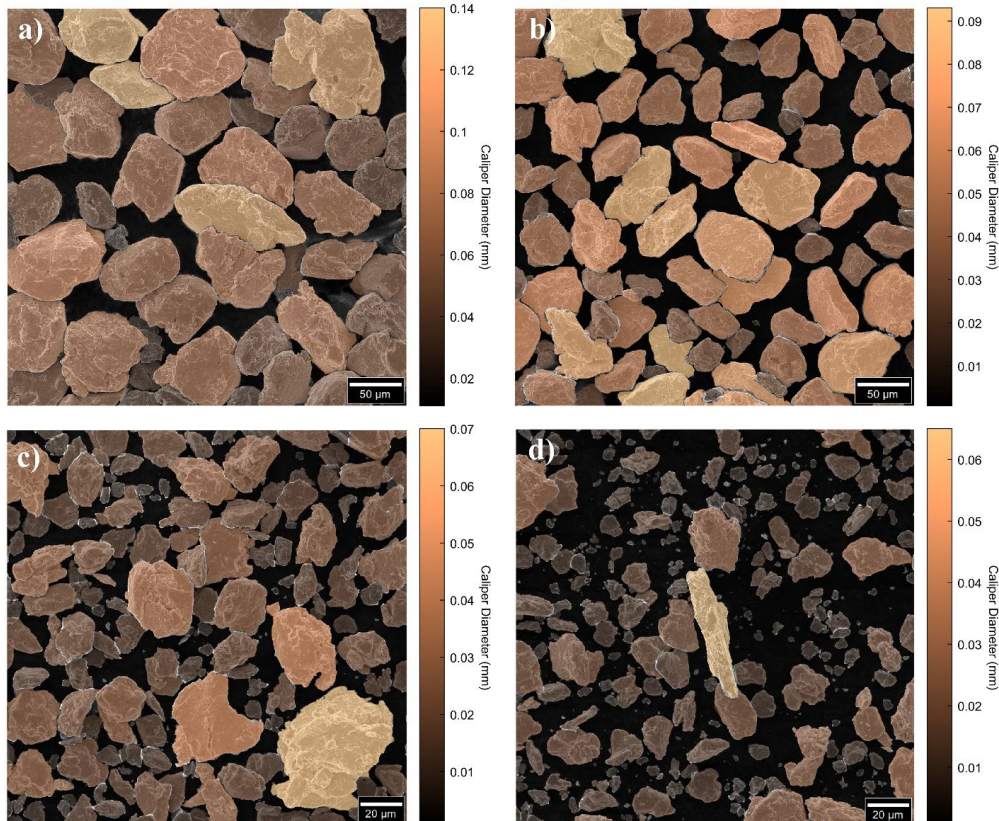


Fig. 1. SEM images given in relation to caliper diameter for Cu-2Zr-0.6B powders after MA time of a) 10 h; b) 20 h; c) 30 h; d) 40 h

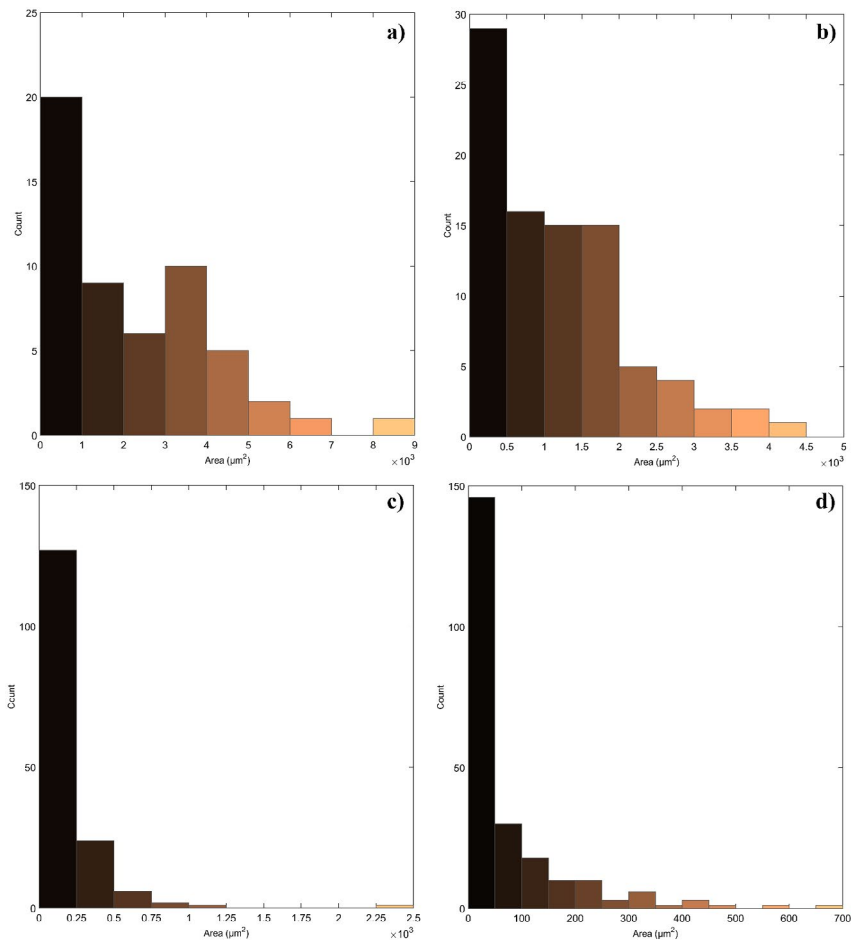


Fig. 2. Histogram showing area analyzed for Cu-2Zr-0.6B powders after MA time of a) 10 h; b) 20 h; c) 30 h; d) 40 h

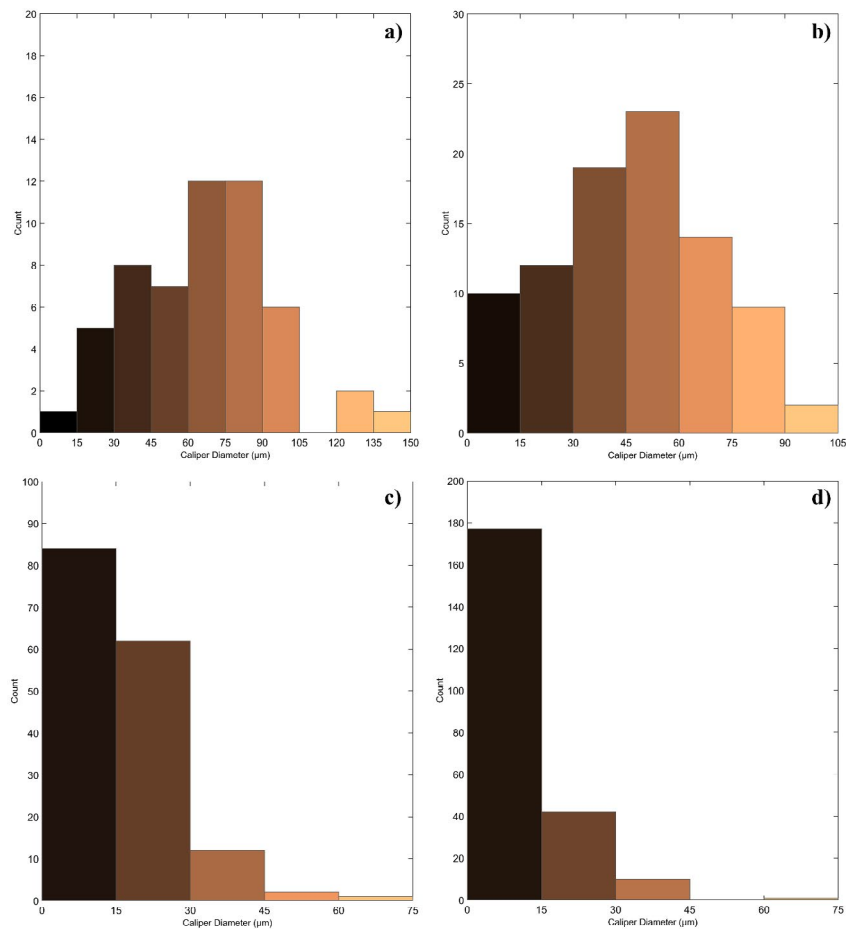


Fig. 3. Histogram showing caliper diameter analyzed for Cu-2Zr-0.6B powders after MA time of a) 10 h; b) 20 h; c) 30 h; d) 40 h

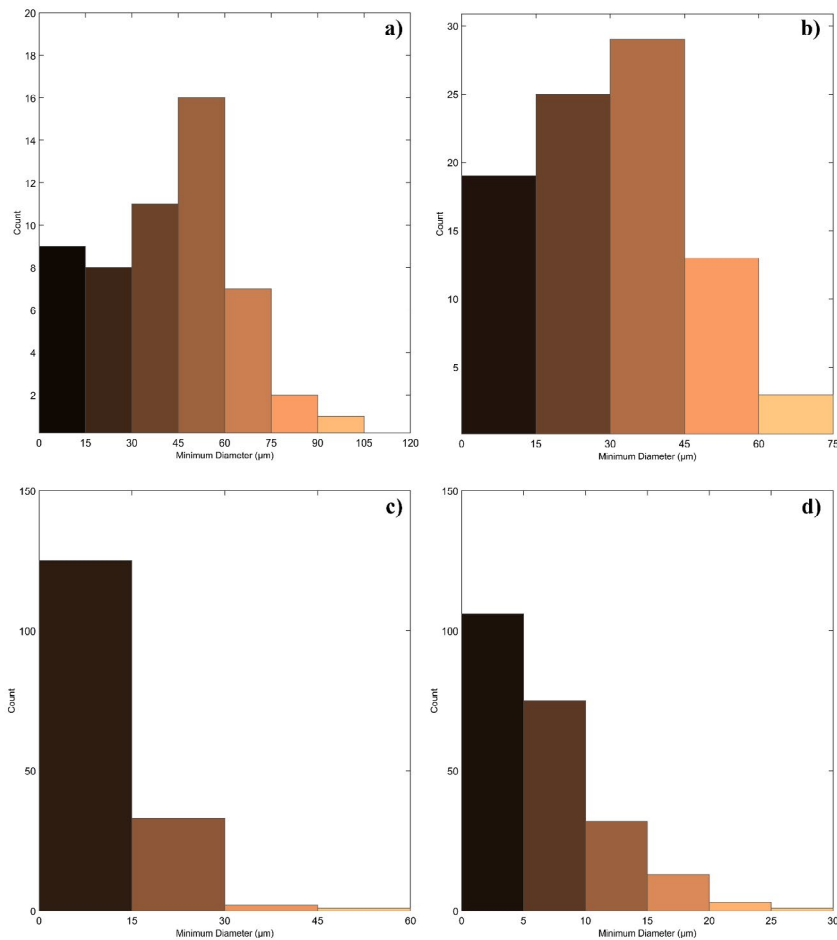


Fig. 4. Histogram showing minimum diameter analyzed for Cu-2Zr-0.6B powders after MA time of a) 10 h; b) 20 h; c) 30 h; d) 40 h

the area of individual particles decreases. For MA of 30 h, we can see that the most particle areas are smaller than  $250 \mu\text{m}^2$ . There are almost no particles with the area size bigger than  $1.500 \mu\text{m}^2$ . For 40 h of MA, the particles area is even smaller with most particles having an area smaller than  $50 \mu\text{m}^2$ . There is a finer distribution of particles ranging from  $50 \mu\text{m}^2$  -  $500 \mu\text{m}^2$ .

Figure 3. shows caliper diameter analyzed for Cu-2Zr-0.6B powders after different MA time. For 10 h of MA it can be seen that most particles have a caliper diameter of around  $75 \mu\text{m}$ . We can see that there are fewer particles with much smaller caliper diameter ( $<20\%$ ), and with much higher caliper diameter ( $<15\%$ ). For 20 h of MA, we can see a finer distribution of the caliper diameter with most particles having the caliper diameter in the range of  $40 \mu\text{m}$  -  $60 \mu\text{m}$ . For 30 h and 40 h of MA, again, the values for caliper diameter are expectedly smaller than  $50 \mu\text{m}$  and  $40 \mu\text{m}$ , respectively.

Figure 4. shows minimum diameter analyzed for Cu-2Zr-0.6B powders after different MA time. Minimum diameter of the most particles MA for 10 h is in the range of  $40 \mu\text{m}$  -  $60 \mu\text{m}$ . For 20 h it reduces to a range of  $30 \mu\text{m}$  -  $40 \mu\text{m}$ . Full range of minimum diameter for particles after 10h of MA is  $0 \mu\text{m}$  -  $120 \mu\text{m}$ , and after 20 h of MA is  $0 \mu\text{m}$  -  $70 \mu\text{m}$ .

The full range reduces after 30 h ( $0 \mu\text{m}$  -  $55 \mu\text{m}$ ) and especially after 40 h ( $0 \mu\text{m}$  -  $25 \mu\text{m}$ ). Most particles after 30 h of MA have a minimum diameter of  $\sim 5 \mu\text{m}$  -  $10 \mu\text{m}$  and for 40 h;  $\sim 5 \mu\text{m}$ .

Figure 5. shows equivalent diameter analyzed for Cu-2Zr-0.6B powders after diff rent MA time. Overall, equivalent diameter decreases with MA time as expected. We can see a fine distribution of particles with equivalent diameter of  $\sim 20 \mu\text{m}$  -  $\sim 80 \mu\text{m}$  for 10 h of MA with the most having an equivalent diameter of  $\sim 60 \mu\text{m}$ . For 20 h of MA, we have a fine distribution between  $0 \mu\text{m}$  -  $\sim 60 \mu\text{m}$ , with the most particles having an equivalent diameter of  $\sim 40 \mu\text{m}$ . After longer MA times, we can see a drastic decrease in equivalent diameter. Most particles after 30 h of MA have an equivalent diameter of around  $10 \mu\text{m}$ , with a range of  $0 \mu\text{m}$  -  $\sim 55 \mu\text{m}$ . After 40 h of MA, most particles have an equivalent diameter within the range of  $0 \mu\text{m}$  -  $\sim 30 \mu\text{m}$ .

## 4. Conclusions

The results indicate that increasing the MA time leads to a progressive reduction in particle size. As MA time increases from 10 h

**Table 1.** Number of particles analyzed and the most common area size [ $\mu\text{m}^2$ ], caliper diameter [ $\mu\text{m}$ ], minimum diameter [ $\mu\text{m}$ ] and equivalent diameter [ $\mu\text{m}$ ] analyzed by MIPAR Image Analysis software for Cu-2Zr-0.6B (wt.%), 10:1 (ball: powder ratio), 10h, 20h, 30h and 40h of mechanical alloying.

Sample	Total particles	Most common size [ $\mu\text{m}^2$ ]	Most common caliper diameter [ $\mu\text{m}$ ]	Most common minimum diameter [ $\mu\text{m}$ ]	Most common equivalent diameter [ $\mu\text{m}$ ]
10h	53	$\sim 1000$	$\sim 75$	$\sim 50$	$\sim 60$
20h	88	$\sim 500$	$\sim 50$	$\sim 35$	$\sim 40$
30h	161	$< 250$	$\sim 15$	$\sim 7.5$	$\sim 10$
40h	231	$< 50$	$\sim 5$	$\sim 5$	$\sim 5$

This data shows that with the increase in milling time, the size of the particles decreases ( $\sim 1000$  to  $< 50$ ), as well as the diameters shown in Table 1. This happens due to the repeated fracturing and cold welding of powder particles inside the high-energy ball mill.

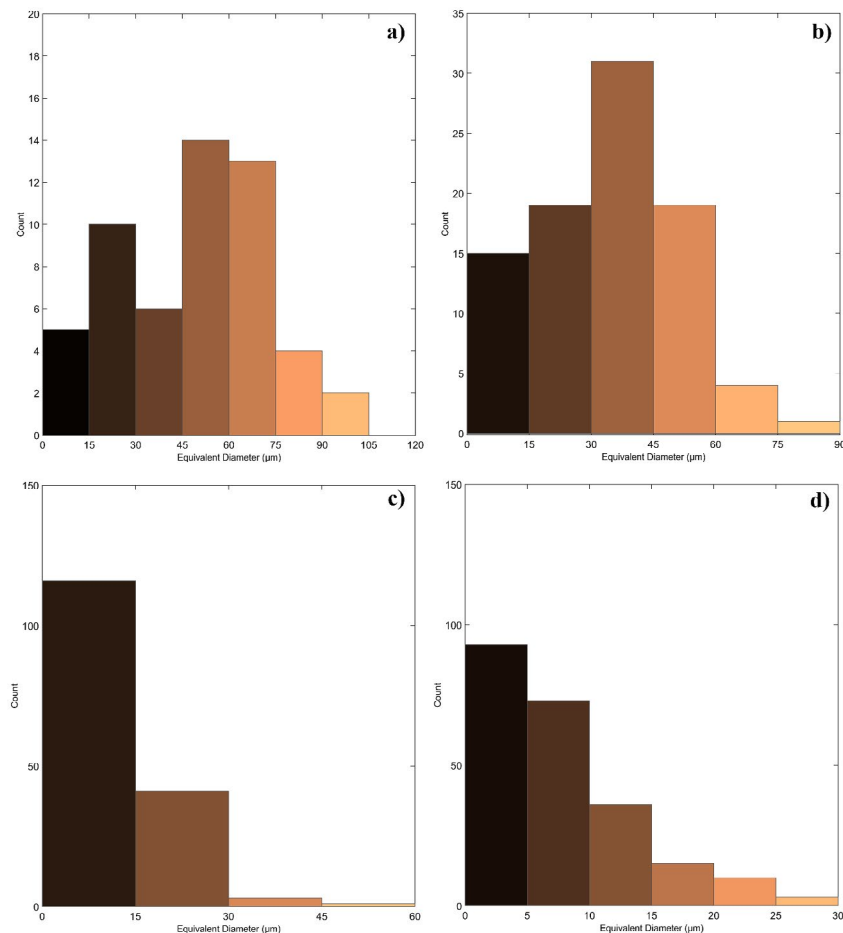


**Fig. 5.** Histogram showing equivalent diameter analyzed for Cu-2Zr-0.6B powders after MA time of a) 10 h; b) 20 h; c) 30 h; d) 40 h

to 4 oh, the particle area significantly decreases, with the majority of particles shifting to smaller size ranges. Similarly, the caliper diameter, minimum diameter, and equivalent diameter exhibit a continuous reduction, reflecting the impact of prolonged MA. It can also be noted that there are more particles in smallest size range as the MA time increases. This suggests that continued MA leads to particle size reduction and more uniform distribution.

## Acknowledgement

This work was funded by the Ministry of Science, Technological Development and Innovations of the Republic of Serbia (Contract No. 451-03-136/2025-03/ 200017, 451-03-136/2025-03/ 200023) and by the Science Fund of the Republic of Serbia, Grant No. 7365, Development of dispersion-strengthened metal-based materials for applications in fusion reactor – DisSFusionMat.

## References

- Akhtar, S., Saad, M., Misbah, R., & Sati, M. C. (2018). Recent Advancements in Powder Metallurgy: A Review. *Materials Today: Proceedings* (Vol. 5), 2214-7853
- Alkindi, Y., Alshammari, Y., Yang, F., & Bolzoni, L. (2023). Joint effect of Zr and Cu on the properties of new powder metallurgy Ti-Zr-Cu alloys. *Materials Science and Engineering: A*, 867, 144708. <https://doi.org/10.1016/J.MSEA.2023.144708>
- Bansal S. A., E., Khanna, V., Gupta, P. (2023). *Metal Matrix Composites; Fabrication, Production, and 3D Printing*, CRC Press.
- Cai, Y., Su, Y., Liu, K., Hua, A., Wang, X., Cao, H., Zhang, D., & Ouyang, Q. (2023). Effect of Sc microalloying on fabrication, microstructure and mechanical properties of SiCp/Al-Cu-Mg-Sc composites via powder metallurgy. *Materials Science and Engineering: A*, 877. <https://doi.org/10.1016/j.msea.2023.145152>
- Chawla, N., & Chawla, K. K. (n.d.). (2016), *Metal Matrix Composites*, Springer Science & Business Media.
- Eessaa, A. K., Elkady, O. A., & El-Shamy, A. M. (2023). Powder metallurgy as a perfect technique for preparation of Cu-TiO<sub>2</sub> composite by identifying their microstructure and optical properties. *Scientific Reports*, 13(1). <https://doi.org/10.1038/s41598-023-33999-y>
- El-Eskandarany, M. Sherif. (2001). *Mechanical alloying for fabrication of advanced engineering materials*. Noyes Publications.
- Gautam, Y. K., Somani, N., Kumar, M., & Sharma, S. K. (2018). A review on fabrication and characterization of copper metal matrix composite (CMMC). *AIP Conference Proceedings*, <https://doi.org/10.1063/1.5058254>
- Jamwal, A., Mittal, P., Agrawal, R., Gupta, S., Kumar, D., Sadasivuni, K. K., & Gupta, P. (2020). Towards sustainable copper matrix composites: Manufacturing routes with structural, mechanical, electrical and corrosion behaviour. *Journal of Composite Materials* 54(19), 2635-2649. SAGE Publications Ltd. <https://doi.org/10.1177/0021998319900655>
- Malaki, M. (2021). An Insight into Metal Matrix Composites with Nano Size Reinforcement. *Encyclopedia of Materials: Composites*, 1, 42-51. Elsevier. <https://doi.org/10.1016/B978-0-12-803581-8.11798-9>
- Paul, M., Alshammari, Y., Yang, F., & Bolzoni, L. (2023). Processing and properties of powder metallurgy Ti-Cu-Nb alloys. *Journal of Alloys and Compounds*, 944, 169041. <https://doi.org/10.1016/J.JALLCOM.2023.169041>
- Pingale, A. D., Owhal, A., Katarkar, A. S., Belgamwar, S. U., & Rathore, J. S. (2021). Recent researches on Cu-Ni alloy matrix composites through electrodeposition and powder metallurgy methods: A review. *Materials Today: Proceedings*, 47, 3301-3308. <https://doi.org/10.1016/j.matpr.2021.07.145>
- Prasad Yadav, T., Manohar Yadav, R., & Pratap Singh, D. (2012). Mechanical Milling: a Top Down Approach for the Synthesis of Nanomaterials and Nanocomposites. *Nanoscience and Nanotechnology*, 2(3), 22-48. <https://doi.org/10.5923/j.nn.20120203.01>
- Ružić, J., Stašić, J., Rajković, V., & Božić, D. (2014). Synthesis, microstructure and mechanical properties of ZrB<sub>2</sub> nano and microparticle reinforced copper matrix composite by in situ processings. *Materials and Design*, 62, 409-415. <https://doi.org/10.1016/j.matdes.2014.05.036>
- Šap, S., Uzun, M., Usca, Ū. A., Pimenov, D. Y., Giasin, K., & Wojciechowski, S. (2021). Investigation on microstructure, mechanical, and tribological performance of Cu base hybrid composite materials. *Journal of Materials Research and Technology*, 15, 6990-7003. <https://doi.org/10.1016/J.JMRT.2021.11.114>
- Shaik, M. A., & Golla, B. R. (2019). Development of highly wear resistant Cu - Al alloys processed via powder metallurgy. *Tribology International*, 136, 127-139. <https://doi.org/10.1016/j.triboint.2019.03.055>

Shaik, M. A., Golla, B. R., & Khaple, S. (2021). Effect of powder processing and alloying additions (Al/ZrB<sub>2</sub>) on the microstructure, mechanical and electrical properties of Cu. *Advanced Powder Technology*, 32(9), 3314–3323. <https://doi.org/10.1016/j.apt.2021.07.012>

Shang, W., Wang, H., Zhao, S., Zhao, X., Xu, H., Lu, H., Chen, D., Fan, B., & Zhang, R. (2014). Processing and properties of ZrB<sub>2</sub>-Cu composites sintered by hot-pressing sintering. *Key Engineering Materials*, 602–603, 447–450. <https://doi.org/10.4028/www.scientific.net/KEM.602-603.447>

Sosa J., Huber D., Welk B., Fraser H. (2014). Development and application of MIPAR™: a novel software package for two- and three-dimensional microstructural characterization, *Integrating Materials and Manufacturing Innovation*, 3(1), 123- 140, <https://doi.org/10.1186/2193-9772-3-10>

Srivatsan, T. S., Pradeep, Rohatgi, K., Murph, S. H. (2022) *Metal-Matrix Composites Advances in Processing, Characterization, Performance and Analysis*, Springer Nature

Suryanarayana, C. (2007). *Mechanical alloying and milling*.

Taha, M. A., Youness, R. A., & Zawrah, M. F. (2019). Review on nanocomposites fabricated by mechanical alloying. *International Journal of Minerals, Metallurgy and Materials* 26(9), 1047–1058. <https://doi.org/10.1007/s12613-019-1827-4>

Wang, Z., Tan, Y., & Li, N. (2023). Powder Metallurgy of Titanium Alloys: A Brief Review. *Journal of Alloys and Compounds*, 171030. <https://doi.org/10.1016/j.jallcom.2023.171030>

Wong-Ángel, W. D., Téllez-Jurado, L., Chávez-Alcalá, J. F., Chavira-Martínez, E., & Verduzco-Cedeño, V. F. (2014). Effect of copper on the mechanical properties of alloys formed by powder metallurgy. *Materials & Design*, 58, 12–18. <https://doi.org/10.1016/J.MATDES.2014.02.002>

Wu, Z., Hu, J., Xin, Z., Qin, L., Jia, Y., & Jiang, Y. (2023). Microstructure and properties of Cu-Zn-Cr-Zr alloy treated by multistage thermo-mechanical treatment. *Materials Science and Engineering: A*, 870. <https://doi.org/10.1016/j.msea.2023.144679>

Zhang, Z., Sheng, Y., Xu, X., & Li, W. (2015). Microstructural Features and Mechanical Properties of in Situ Formed ZrB<sub>2</sub>/Cu Composites. *Advanced Engineering Materials*, 17(9), 1338–1343. <https://doi.org/10.1002/adem.201400532>